Supporting Information

Facile Fabrication of Three-Dimensional Graphene and Metal-Organic Framework Composites and Their Derivatives for Flexible All-Solid-State Supercapacitors

Xilian Xu,[†,‡] Wenhui Shi,[±,‡] Peng Li,[†] Shaofeng Ye,[†] Chenzeng Ye,[±] Huijian Ye,[†] Tiemei Lu,[†] Aiai Zheng,[†] Jixin Zhu,[§] Lixin Xu,[†] Mingqiang Zhong[†] and Xiehong Cao*,[†]

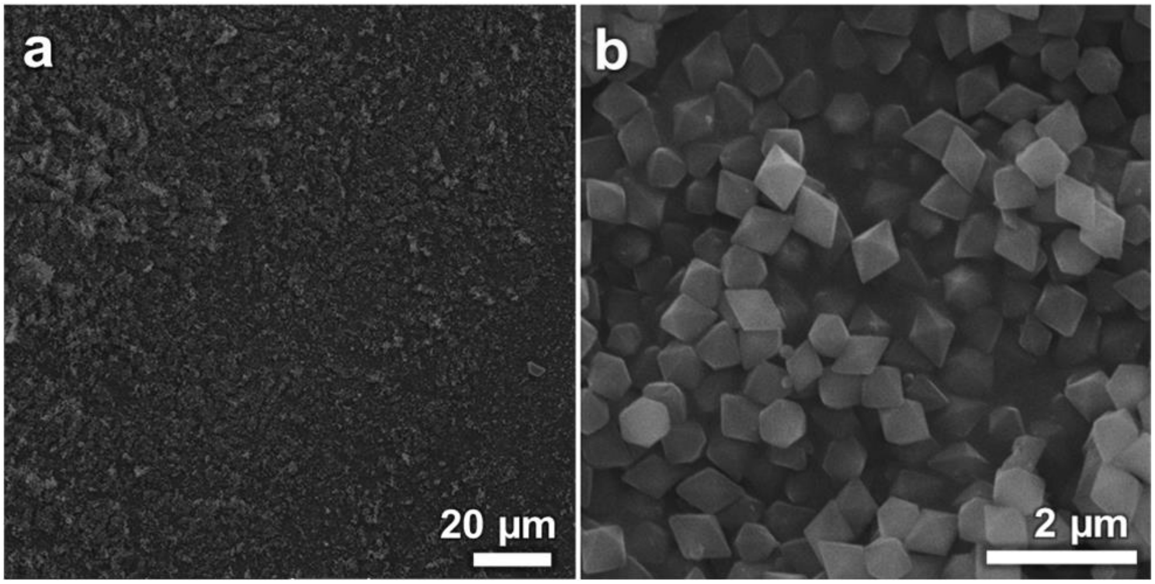

Figure S1. SEM images of Fe-MOF crystals.

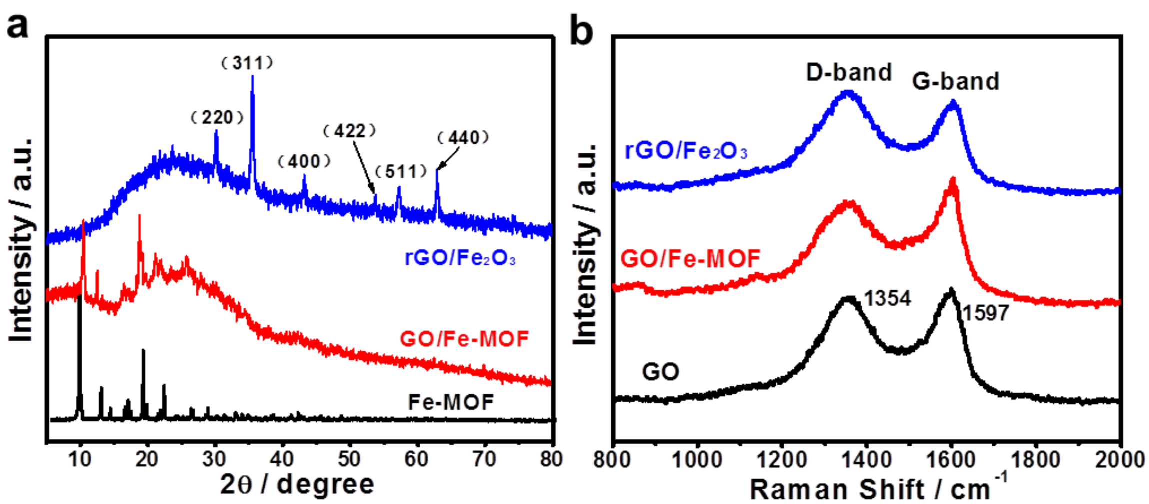

Figure S2. (a) XRD patterns of Fe-MOF crystals, GO/Fe-MOF and rGO/Fe_2O_3 composite aerogels. (b) Raman spectra of GO, GO/Fe-MOF and rGO/Fe_2O_3 composites.

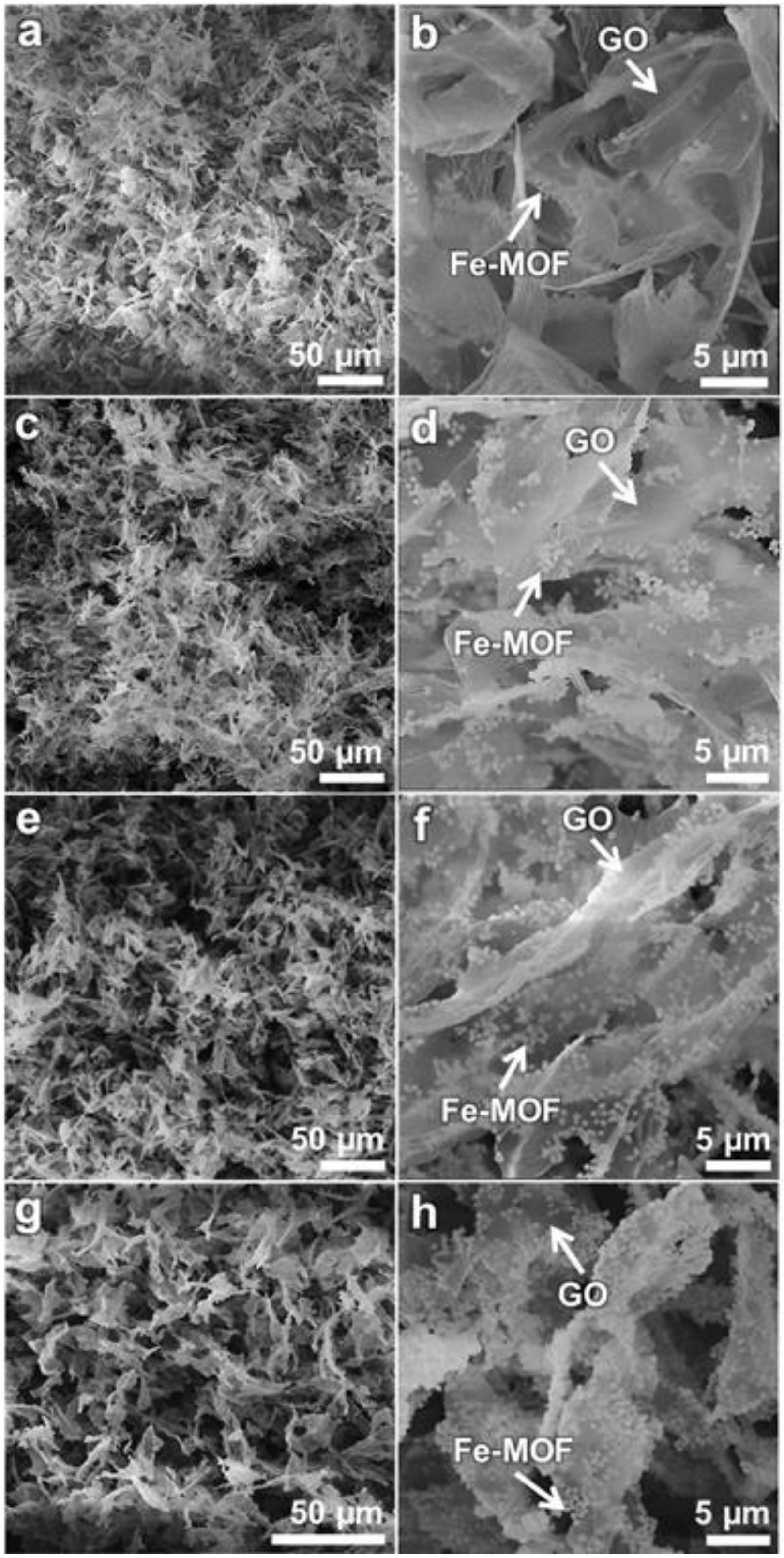

Figure S3. SEM images of GO/Fe-MOF composite aerogels with different weight ratios. (a, b) Fe-MOF : GO = 1 : 1. (c, d) Fe-MOF : GO = 2 : 1. (e, f) Fe-MOF : GO = 4 : 1. (g, h) Fe-MOF : GO = 5 : 1.

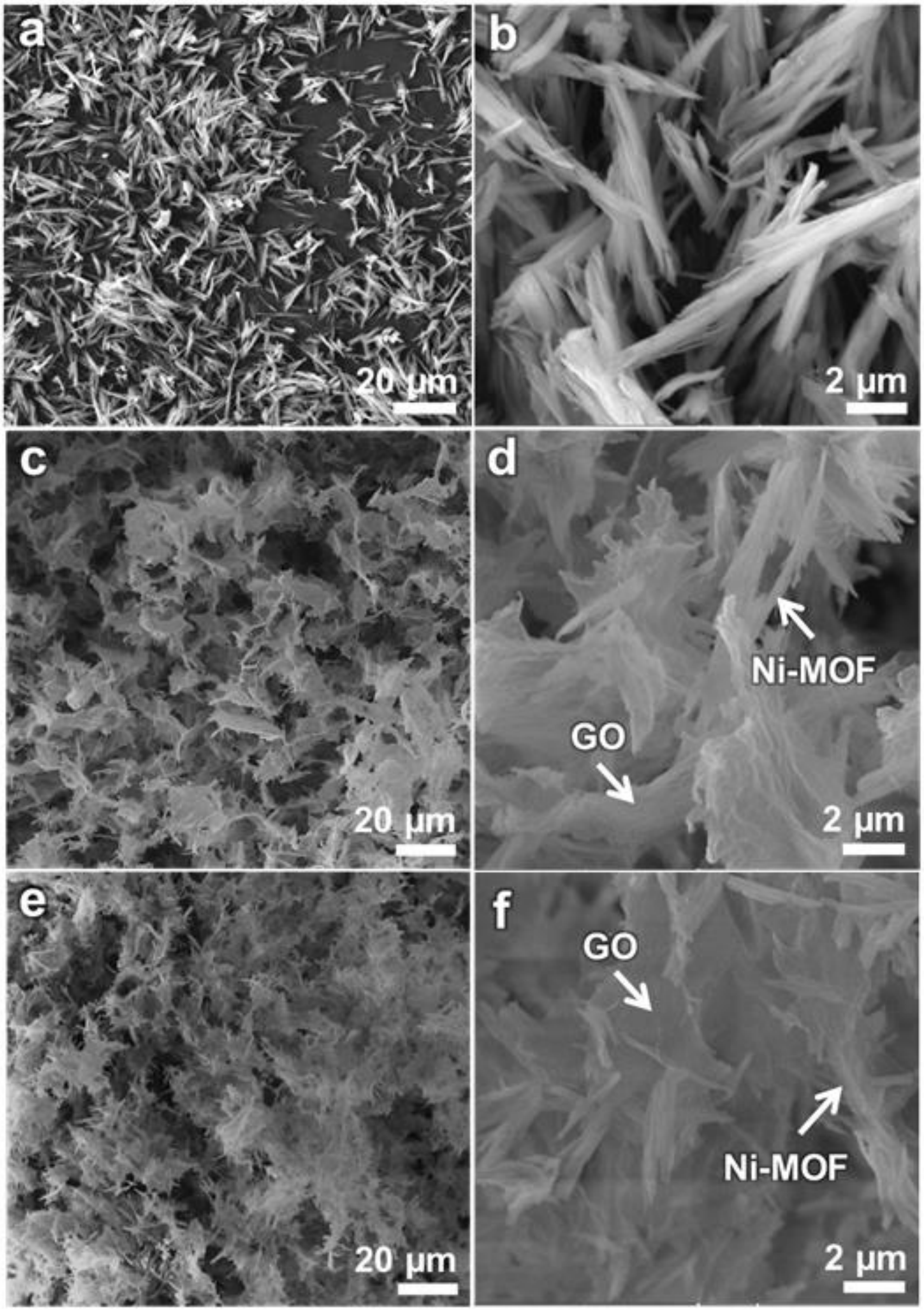

Figure S4. SEM images of (a, b) Ni-MOF crystals and (c-f) GO/Ni-MOF composite aerogels with different weight ratios. Ni-MOF : GO = 1 : 1 (c, d) and 3 : 1 (e, f).

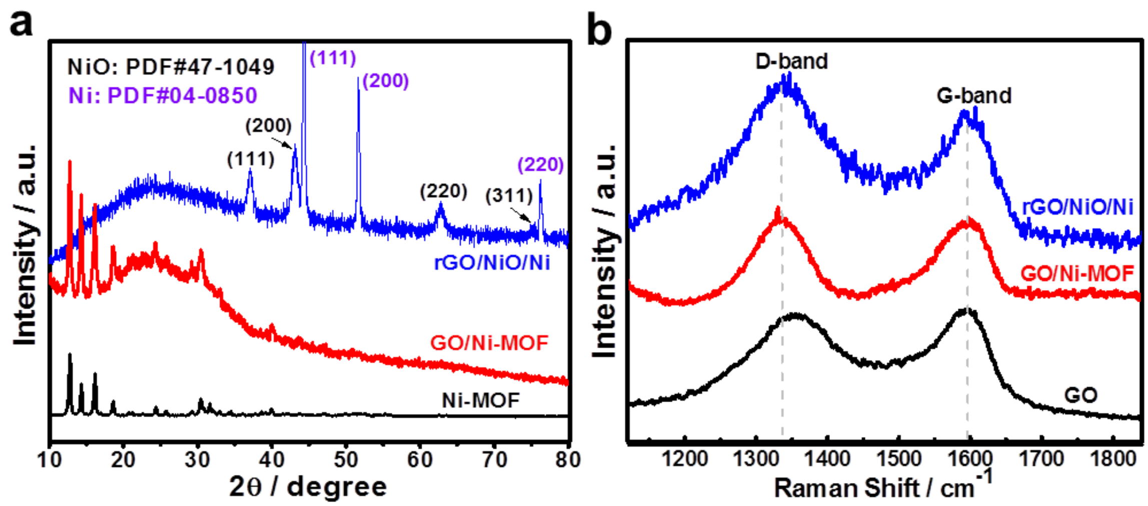

Figure S5. (a) XRD patterns of Ni-MOF crystals, GO/Ni-MOF and rGO/NiO/Ni composites. (b) Raman spectra of GO, GO/Ni-MOF and rGO/NiO/Ni composites.

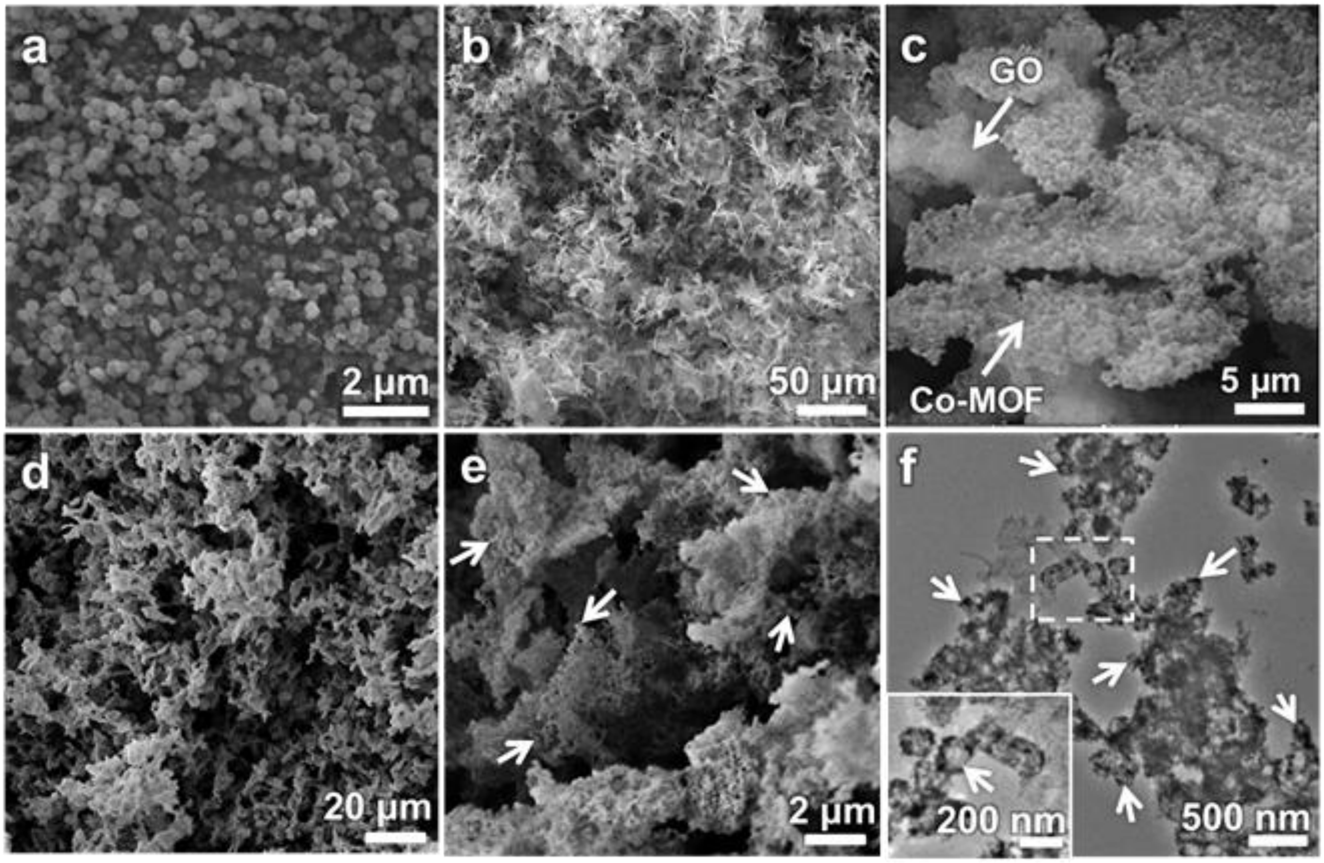

Figure S6. SEM images of (a) Co-MOF crystals, and (b-e) the GO/Co-MOF composite aerogels (weight ratio of Co-MOF to GO is 15 : 1) before (b,c) and after (d,e) the two-step annealing process. (f) TEM image of the rGO/Co-MOF-derived composite. Inset: High-magnification TEM image of the rectangular range in (f). The arrows in (e,f) indicate the Co-MOF-derived structures.

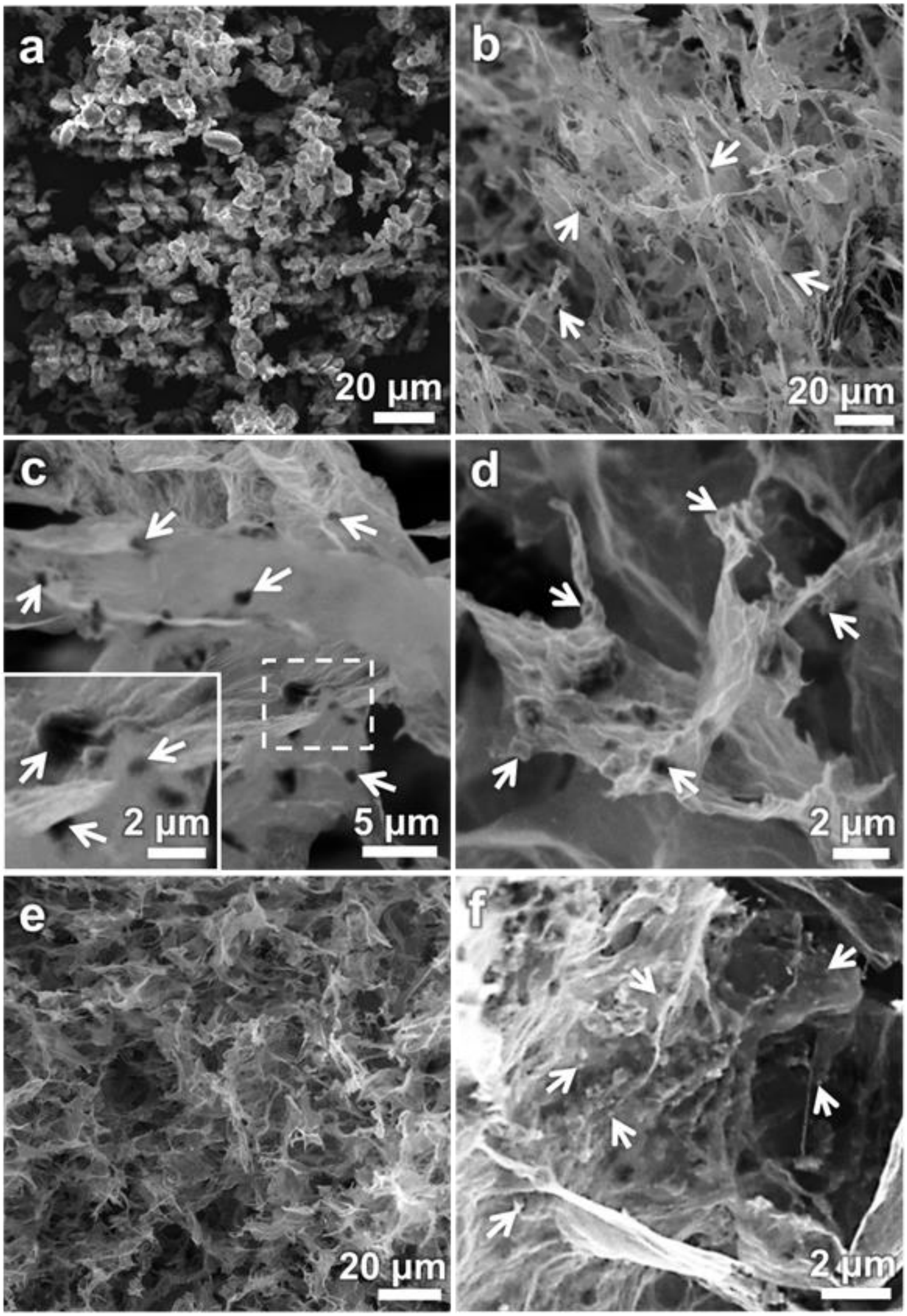

Figure S7. SEM images of (a) Sn-MOF crystals, and (b-f) the GO/Sn-MOF composite aerogels (weight ratio of Sn-MOF to GO is 5 : 1) before (b-d) and after (e,f) the two-step annealing process. Inset in (c): High-magnification SEM image of the rectangular range in (c). The arrows indicate the Sn-MOF crystals (b-d) and Sn-MOF-derived materials (f).

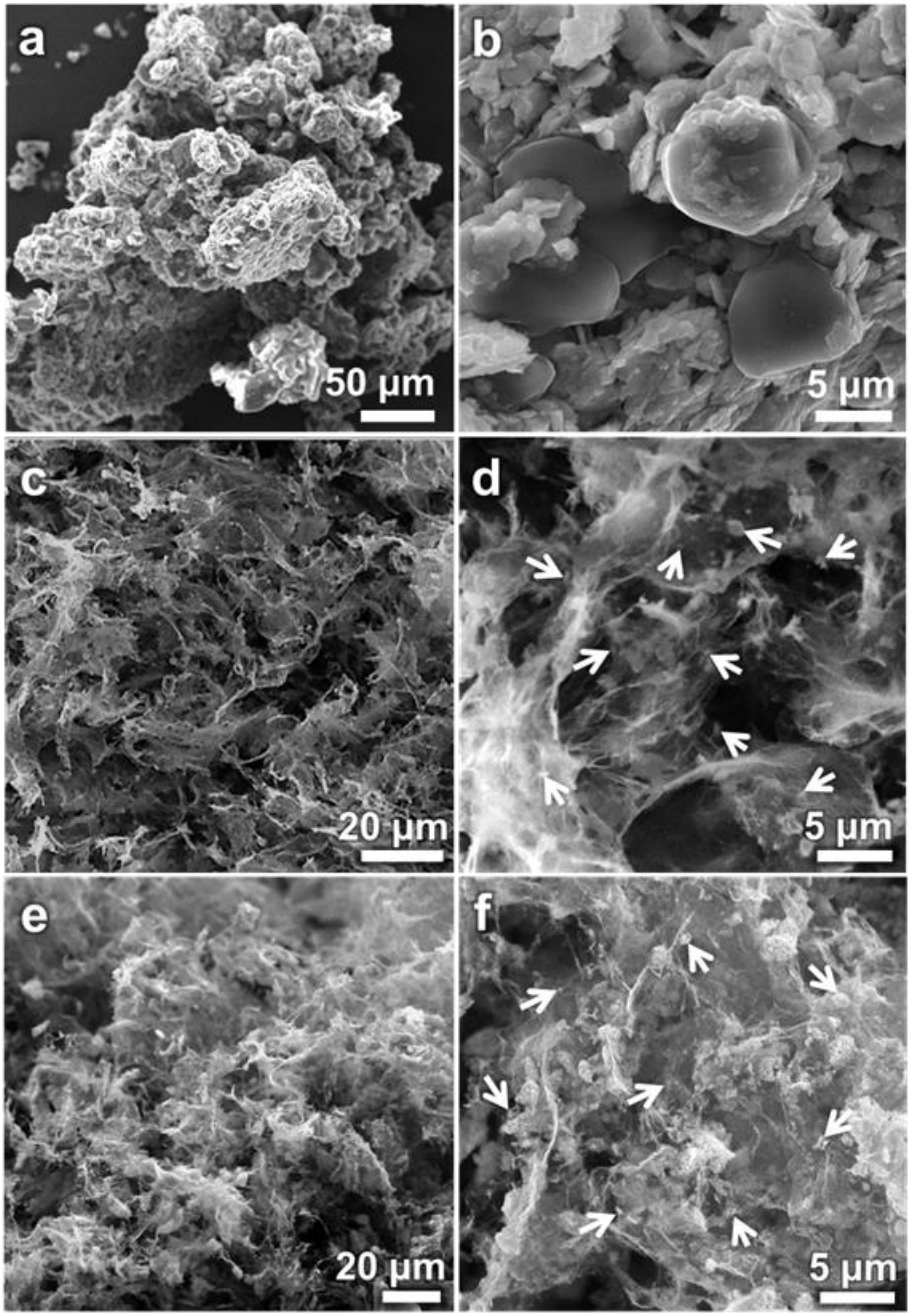

Figure S8. SEM images of (a,b) ZIF-8 crystals, and (c-f) the GO/ZIF-8 composite aerogels (weight ratio of ZIF-8 to GO is 5 : 1) before (c,d) and after (e,f) the two-step annealing process. The arrows indicate the ZIF-8 crystals (d) and ZIF-8-derived materials (f).

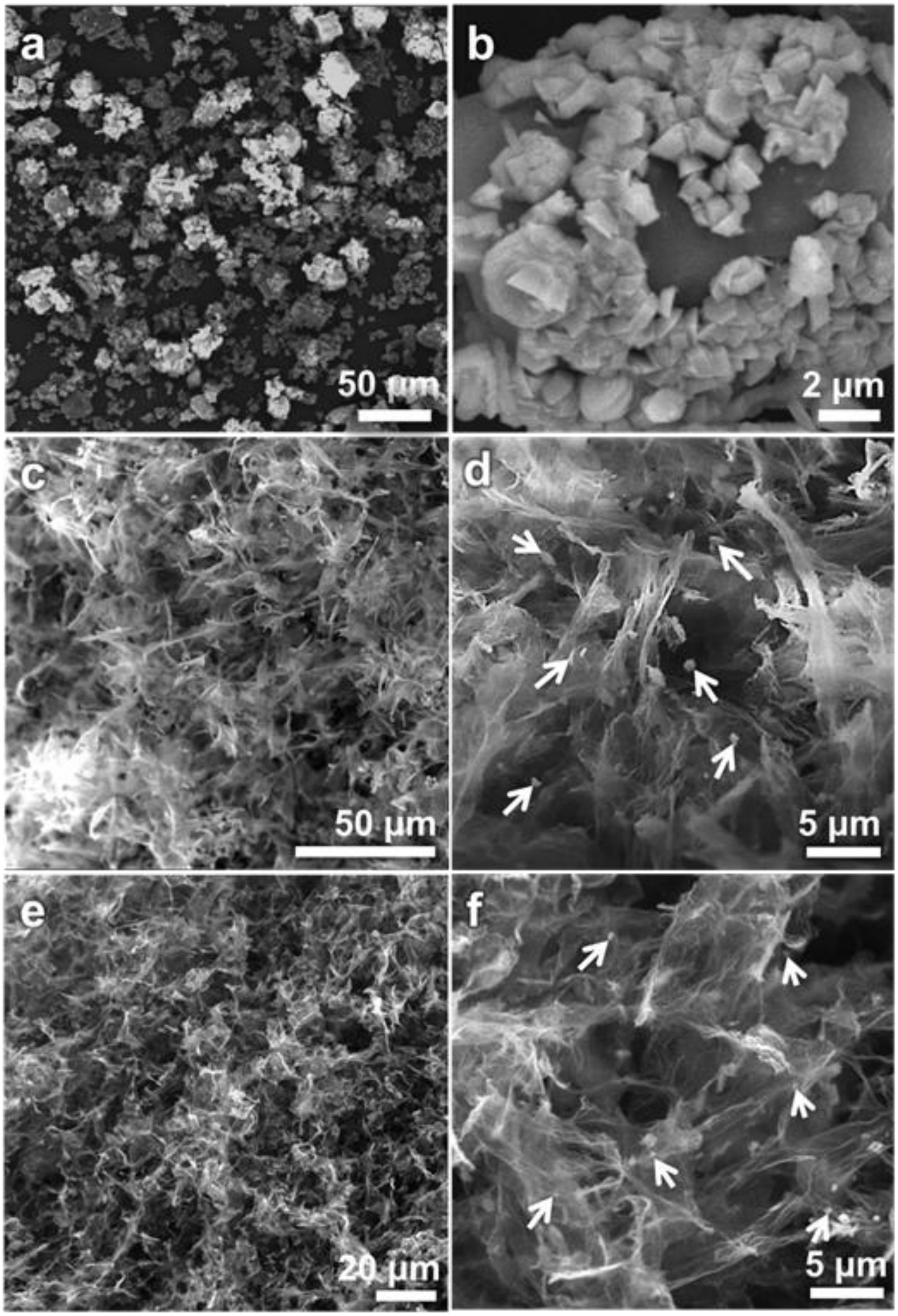

Figure S9. SEM images of (a,b) MOF-5 crystals and (c-f) the GO/MOF-5 composite aerogels (weight ratio of MOF-5 to GO is 5 : 1) before (c,d) and after (e,f) the two-step annealing process. The arrows indicate the MOF-5 crystals (d) and MOF-5-derived materials (f).

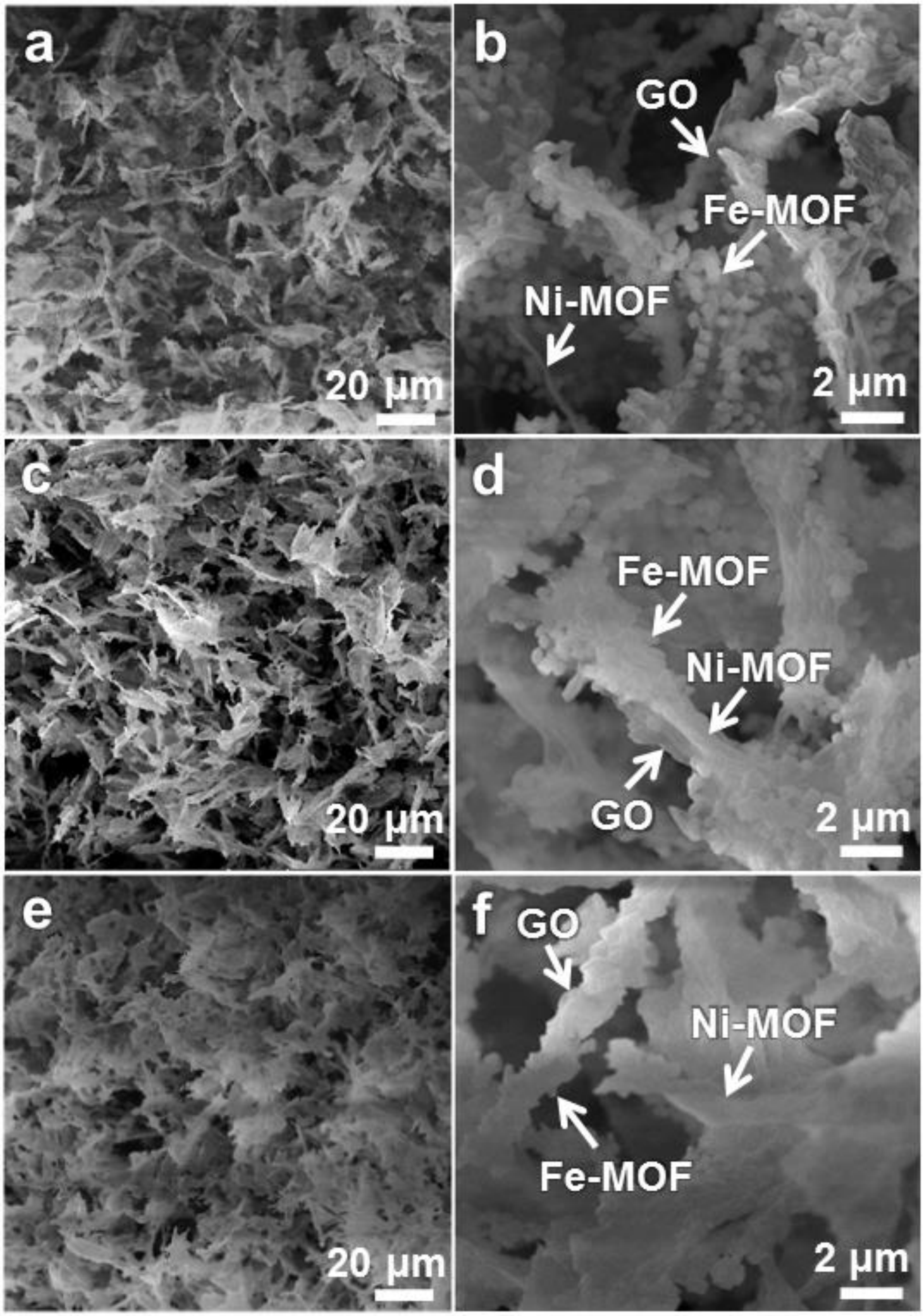

Figure S10. SEM images of GO/Fe-MOF/Ni-MOF composite aerogels with different weight ratios. Fe-MOF : Ni-MOF : GO = 5 : 1 :1 (a, b), 5 : 3 : 1 (c, d), and 5 : 5 : 1 (e, f).

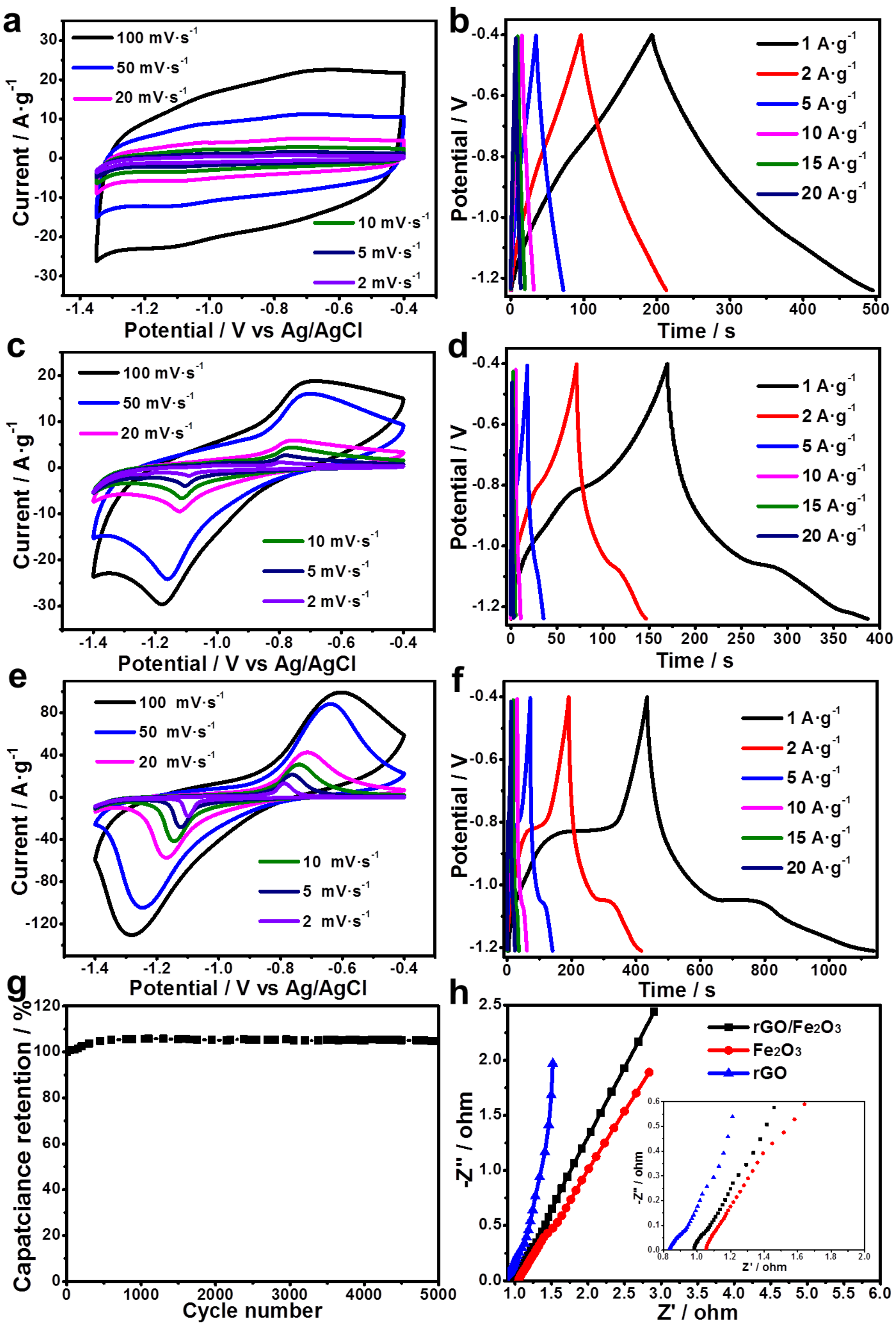

Figure S11. Electrochemical performance of the obtained rGO/Fe_2O_3, rGO and Fe_2O_3. The CV and charge/discharge curves of (a,b) rGO, (c,d) Fe_2O_3, and (e,f) rGO/Fe_2O_3 electrodes. (g) Cycling performance of rGO/Fe_2O_3 composite electrode measured by charging and discharging it at 20 $A \cdot g^{-1}$ for 5000 cycles. (h) Nyquist plots of rGO/Fe_2O_3, Fe_2O_3 and rGO electrodes.

The CV curves of rGO/Fe_2O_3 and Fe_2O_3 electrodes show a pair of well-defined peaks at around -0.7 and -1.2 V, which are attributed to the reversible oxidation and reduction processes of $Fe^{2+} \leftrightarrow Fe^{3+}$.[S1] The CV curves of the rGO/Fe_2O_3 composites exhibit no obvious distortion of shapes at higher scan rates, suggesting good rate capability and rapid diffusion of electrolyte ions into the composite (Figure S11e). Figure S11g shows the *Cs* of rGO/Fe_2O_3 composite increased in the first 500 cycles. This could be due to the gradually penetration of electrolyte ions into the rGO/Fe_2O_3 composite electrode.[S2] The *Cs* of the composite electrode shows no obvious change in the subsequent 4500 cycles.

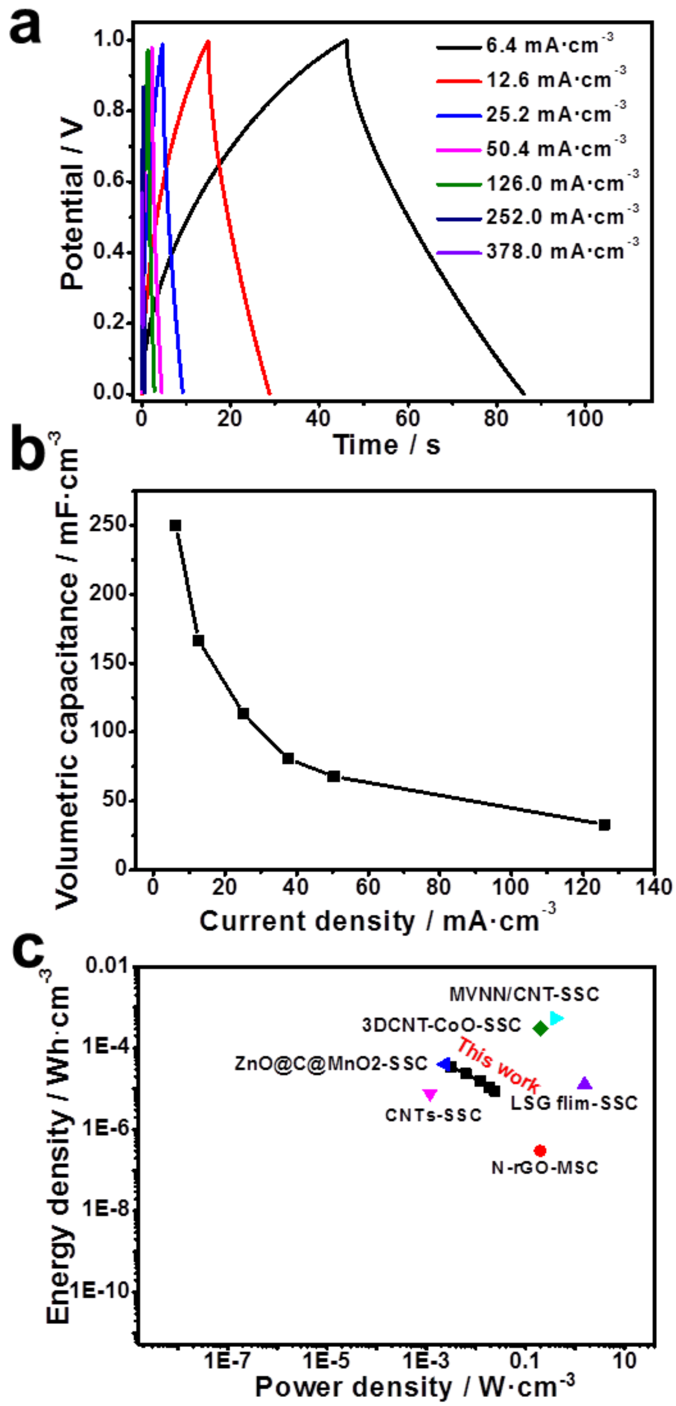

Figure S12. (a) Charge/discharge curves of the all-solid-state symmetric supercapacitor device fabricated using rGO/Fe_2O_3 composite at different current densities. (b) Volumetric capacitance at different current densities. (c) The Ragone plots of the fabricated device, and the comparison of our performance with previous reports.

Table S1. The comparison of electrochemical performance of graphene/Fe_2O_3 composite-based electrodes in various aqueous electrolytes.

Materials	**Morphology of Fe_2O_3**	**Specific capacitance (F/g)**	**Rate capability (F/g)**	**Cycling performance**	**Electrolyte**	**Ref**
Graphene/Fe_2O_3	particles	908 at 2 A/g	626 at 50 A/g	75% after 200 cycles at 20 mV/s	1 M KOH	S1
Fe_2O_3 QDs/FGS	quantum dots	347 at 10 mV/s	140 at 1600 mV/s	95% after 5000 cycles at 0.5 A/g	1 M Na_2SO_4	S3
α-Fe_2O_3 NTs-rGO	nanotubes	181 at 3 A/g	69 at 10 A/g	110% after 2000 cycles at 5 A/g	0.1 M K_2SO_4	S4
NGFeCs	particles	260 at 2A/g	110 at 7 A/g	82.5% after 1000 cycles at 2 A/g	1 M Na_2SO_4	S5
NR-rGO	nanorods	504 at 2 mA/cm^2	Not reported	Not reported	1 M Na_2SO_4	S6
Fe_2O_3–graphene	particles	226 at 1 A/g	90.8 at 5A/g	Not reported	1 M Na_2SO_4	S7
GNS/Fe_2O_3	nanorods	320 at 10 mA/cm^2	152 at 100 mA/cm^2	97% after 500 cycles at 10 mA/cm^2	6 M KOH	S8
Fe_2O_3–graphene	nanoparticles	151.8 at 1 A/g	94 at 16 A/g	86% after 1000 cycles at 2 A/g	2 M KOH	S9
Fe_2O_3/NrGO	nanoparticles	618 at 0.5 A/g	350 at 10 A/g	56.7% after 5000 cycles at 4 A/g	1 M KOH	S10
Fe_2O_3/rGOA	nanoparticles	627 at 1 A/g	522 at 20 A/g	57% after 1500 cycles at 5 A/g	2 M KOH	S11
Fe_2O_3 NDs@NG	nanodots	274 at 1 A/g	140 at 50 A/g	75.3% after 100000 cycles at 5 A/g	1 M KOH	S12
Fe_2O_3/GH	nanoparticles	1111 at 5 A/g	615 at 100 A/g	46.8% after 5000 cycles at 20 mV/s	6 M KOH	S13
G-Fe_2O_3	nanoparticles	1095 at 3 A/g	506.6 at 30 A/g	91.1% after 1 000 cycles at 10 A/g	3 M KOH	S14
Fe_2O_3/GA	nanoparticles	81.3 at 1 A/g	62.7 at 10 A/g	Not reported	0.5 M Na_2SO_4	S15
α-Fe_2O_3/rGO	nanoplates	903 at 1 A/g	Not reported	70% after 1000 cycles at 5 A/g	1 M KOH	S16
Fe_2O_3/rGO	nanoplates	1083 at 2 A/g	199 at 20 A/g	75.3% after 1000 cycles at 4 A/g	1 M KOH	S17
γ-Fe_2O_3/graphene	spheres	332.7 at 2 A/g	98.9 at 10 A/g	95% after 2000 cycles at 10 A/g	1 M KOH	S18
rGO/Fe_2O_3	**porous structure assembled by particles**	**869.2 at 1 A/g**	**289.6 at 20 A/g 362.5 at 10 A/g 431.1 at 5 A/g**	**105.1% after 5000 cycles at 20 A/g**	**6 M KOH**	**This work**

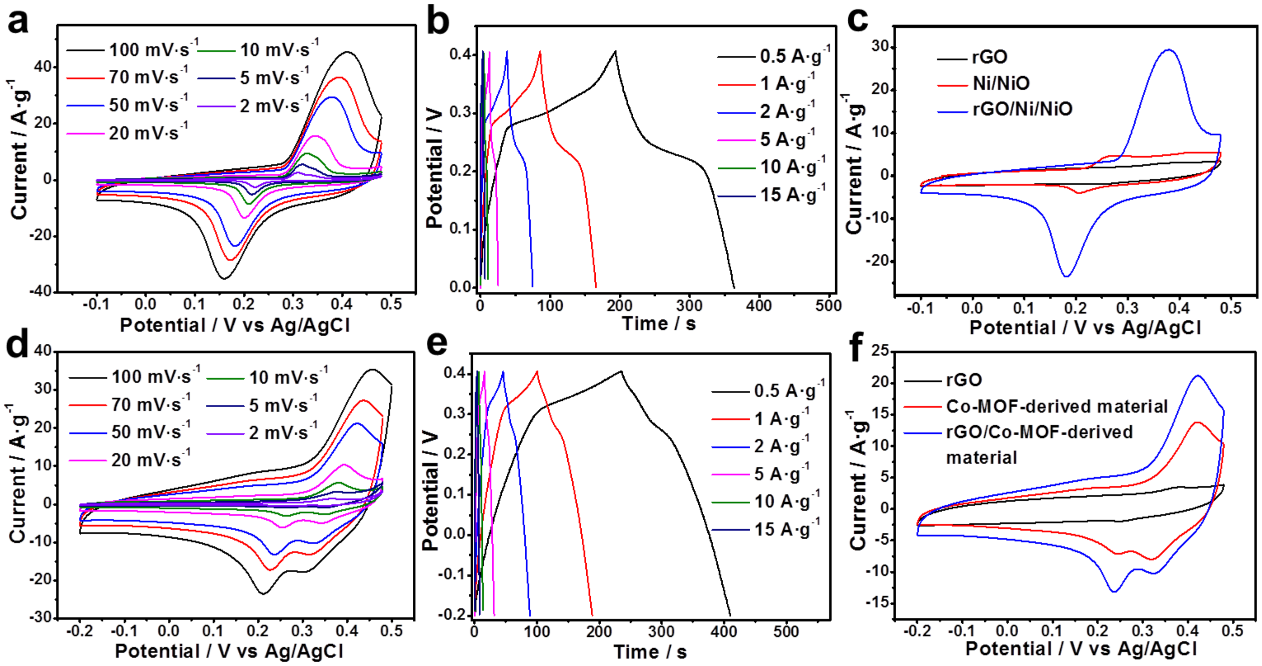

Figure S13. Electrochemical performances of the (a,b) rGO/Ni/NiO and (d,e) rGO/Co-MOF-derived composite aerogels. Comparison of electrochemical performance of the (c) rGO/Ni/NiO and (f) rGO/Co-MOF-derived composite aerogels with their corresponding individual counterparts (scan rate = 50 $mV \cdot s^{-1}$).

REFERENCES

(S1) Wang, H.; Xu, Z.; Yi, H.; Wei, H.; Guo, Z.; Wang, X. One-step preparation of single-crystalline Fe_2O_3 particles/graphene composite hydrogels as high performance anode materials for supercapacitors. *Nano Energy* **2014**, *7*, 86-96.

(S2) Zhang, C.; Qian, L. H.; Zhang, K.; Yuan, S. L.; Xiao, J. W.; Wang, S. Hierarchical porous Ni_NiO core–shells with superior conductivity for electrochemical pseudo-capacitors and glucose sensors. *J. Mater. Chem. A* **2015**, *3*, 10519–10525

(S3) Xia, H.; Hong, C. Y.; Li, B.; Zhao, B.; Lin, Z. X.; Zheng, M. B.; Savilov, S. V.; Aldoshin, S. M. Facile Synthesis of Hematite Quantum-Dot/Functionalized Graphene-Sheet Composites as Advanced Anode Materials for Asymmetric Supercapacitors. *Adv. Funct. Mater.* **2015**, *25*, 627–635

(S4) Lee, K. S. D.; Fan, H. M.; Mhaisalkar, S.; Tan, H. R.; Tok, E. S.; Loh, K. P.; Chin,W. S.; Sow, C. H. α-Fe_2O_3 nanotubes-reduced graphene oxide composites as synergistic electrochemical capacitor materials. *Nanoscale* **2012**, *4*, 2958–2961.

(S5) Zhao, P.; Li, W.; Wang, G.; Yu, B.; Li, X.; Bai, J.; Ren, Z. Facile hydrothermal fabrication of nitrogen-doped graphene/Fe_2O_3 composites as high performance electrode materials for supercapacitor. *J. Alloy. Compd.* **2014**, *604*, 87-93.

(S6) Low, Q. X.; Ho, G. W. Facile structural tuning and compositing of iron oxide-graphene anode towards enhanced supacapacitive performance. *Nano Energy* **2014**, *5*, 28-35.

(S7) Wang, Z.; Ma, C.; Wang, H.; Liu, Z.; Hao, Z. Facilely synthesized Fe_2O_3–graphene nanocomposite as novel electrode materials for supercapacitors with high performance. *J. Alloy. Compd.* **2013**, *552*, 486-491.

(S8) Yang, W.; Gao, Z.; Wang, J.; Wang, B.; Liu, L. Hydrothermal synthesis of reduced graphene sheets/Fe_2O_3 nanorods composites and their enhanced electrochemical performance for supercapacitors. *Solid State Sci.* **2013**, *20*, 46-53.

(S9) Wang, D.; Li, Y.; Wang, Q.; Wang, T. Nanostructured Fe_2O_3–graphene composite as a novel electrode material for supercapacitors. *J. Solid State Electr.* **2011**, *16*, 2095-2102.

(S10) Ma, Z.; Huang, X.; Dou, S.; Wu, J.; Wang, S. One-Pot Synthesis of Fe_2O_3 Nanoparticles on Nitrogen-Doped Graphene as Advanced Supercapacitor Electrode Materials. *J. Phy. Chem. C* **2014**, *118*, 17231-17239.

(S11) Song, Z.; Liu, W.; Wei, W.; Quan, C.; Sun, N.; Zhou, Q.; Liu, G.; Wen, X. Preparation and electrochemical properties of Fe_2O_3/reduced graphene oxide aerogel (Fe_2O_3/rGOA) composites for supercapacitors. *J. Alloy. Compd.* **2016**, *685*, 355-363.

(S12) Liu, L.; Lang, J.; Zhang, P.; Hu, B.; Yan, X. Facile Synthesis of Fe_2O_3 Nano-Dots@Nitrogen-Doped Graphene for Supercapacitor Electrode with Ultralong Cycle Life in KOH Electrolyte. *ACS Appl. Mater. Inter.* **2016**, *8*, 9335-9344.

(S13) Zhang, H.; Gao, Q.; Yang, K.; Tan, Y.; Tian, W.; Zhu, L.; Yang, C. Solvothermally induced α-Fe_2O_3_graphene nanocomposites with ultrahigh capacitance and excellent rate capability for supercapacitors. *J. Mater. Chem. A* **2015**, *3*, 22005–22011

(S14) Chen, J.; Xu, J.; Zhou, S.; Zhao, N.; Wong, C.-P. Template-grown graphene/porous Fe_2O_3 nanocomposite: A high-performance anode material for pseudocapacitors. *Nano Energy* **2015**, *15*, 719-728.

(S15) Song, Z.; Liu, W.; Xiao, P.; Zhao, Z.; Liu, G.; Qiu, J. Nano-iron oxide (Fe_2O_3)/three-dimensional graphene aerogel composite as supercapacitor electrode materials with extremely wide working potential window. *Mater. Lett.* **2015**, *145*, 44-47.

(S16) Quan, H.; Cheng, B.; Xiao, Y.; Lei, S. One-pot synthesis of α-Fe_2O_3 nanoplates-reduced graphene oxide composites for supercapacitor application. *Chem. Eng. J.* **2016**, *286*, 165-173.

(S17) Gao, Y.; Wu, D.; Wang, T.; Jia, D.; Xia, W.; Lv, Y.; Cao, Y.; Tan, Y.; Liu, P. One-step solvothermal synthesis of quasi-hexagonal Fe_2O_3 nanoplates/graphene composite as high performance electrode material for supercapacitor. *Electrochim. Acta* **2016**, *191*, 275-283.

(S18) Liu, Y.; Liu, F.; Chen, Y.; Jiang, J.; Ai, Y.; Han, S.; Lin, H. Self-assembled graphene coupled hollow-structured γ-Fe_2O_3 spheres with crystal of transition for enhanced supercapacitors. *RSC Adv.* **2016**, *6*, 23659–23665.